Chemical composition evaluation and pyrolysis behavior of biomass tar: Pyrolysis experiment and kinetic studies

Weijuan Lan, Yunlong Zhou, Jiaxin Liu, Yingxian Wang, Dongxue Yin, Jiangtao Ji, Xin Jin*

(*School of Agricultural Equipment Engineering, Henan University of Science and Technology, Luoyang 471003, Henan, China*)

Abstract: Biomass gasification process generates the residual tar, which in turn exerts some negative influence on biomass gasification system. To reduce this harmful influence, an evaluation of the tar properties during the biomass gasification was studied. The chemical composition and pyrolysis behavior of biomass tar were investigated. The complex chemical composition of the tar, which includes phenol derivatives, naphthalene derivatives, other macromolecular aromatic compounds, furans, and other compounds (carbon number from 7 to 14), was established by gas chromatography-mass spectrometry technique. Thermogravimetric analysis was performed with two heating rates (10°C/min and 20°C/min), and Coats-Redfern method was applied to assess the kinetic parameters, i.e., the activation energy (E) and pre-exponential factor (A) of tar thermo-chemical decomposition. The results showed that the main degradation of tar is a two-step process, including a volatilization step at lower temperatures (<105°C) and a pyrolysis step at higher temperatures (105°C-380°C). The application of the Coats-Redfern method revealed a variation trend of the activation energy during the decomposition of tar in a non-isothermal model. It shows that high temperature is more conducive to tar pyrolysis. By adjusting the temperature to control the generation and removal of tar, new approaches are provided for designing and optimizing biomass gasification systems.

Keywords: biomass tar, chemical components, thermogravimetric analysis, kinetics

DOI: 10.25165/j.ijabe.20241703.8362

Citation: Lan W J, Zhou Y L, Liu J X, Wang Y X, Yin D X, Ji J T, et al. Chemical composition evaluation and pyrolysis behavior of biomass tar: Pyrolysis experiment and kinetic studies. Int J Agric & Biol Eng, 2024; 17(3): 230–234.

1 Introduction

Biomass gasification is one of the major techniques by which high-quality gases that can be used for subsequent gas supply, heating, power generation, and gas synthesis are obtained[1-4]. Tar is a by-product of biomass gasification consisting of aromatic compounds (from monocyclic to pentacyclic compounds), hydrocarbons, other complex polycyclic aromatic hydrocarbons (PAHs), and so forth[5-9]. The presence of tar has a negative influence on the efficient use of gases generated by biomass gasification. Additionally, it plugs, contaminates, and corrodes the gas pipelines, adversely affects the gas stoves, shortens the service life of the equipment, and restricts the normal operation of the gasification system[10-12]. When the gases generated by biomass gasification are used for power generation or gas supply, the negative impact of tar makes these operations impossible, and may also give rise to secondary contamination[13-15]. Tar is also an environmental hazard (toxic and carcinogenic) and usually co-exists with water during biomass gasification[16-18]. Therefore, the removal of dry tar by an efficient method is essential for commercializing biomass gasification[19-21].

The presence of tar also affects the commercial promotion and applications of biomass gasification[22-25]. Therefore, it is important to have a clear understanding of the characteristics of tar to provide a basis for the utilization of tar as a valuable resource[26-29]. Thus, many studies on the chemical composition of tar and its thermal behavior evaluated by thermogravimetry and other techniques were reported[30-33]. Chen et al.[34] studied the tar adhering to the furnace by thermo-gravimetric analysis (TGA) after the pine bark was gasified in the water-cooled biomass pyrolysis gasifier. Wang et al.[35] used gas chromatography-mass spectrometer (GC-MS) technique to analyze biomass tar and its chemical composition, and found that the biomass and its fractions include many valuable chemical compounds, and the main components of biomass tar are similar to those of diesel. Xie et al.[36] used a TG analyzer to investigate the characteristics of tar combustion in oil fume tunnels in the catering industry at five heating rates. Karaosmanoglu et al.[37] verified if the characteristics of tar recommend it as a fuel, and found that tar has a high carbon content, but low ash, sulfur, and nitrogen contents.

In this study, the chemical composition of tar was analyzed by GC-MS, and the pyrolysis behavior was determined based on TG analysis. The activation energy (E), and frequency factor (A), were determined from the TG-derivative thermogravimetry (TG-DTG) data using two heating rates, 10°C/min and 20°C/min. The kinetic parameters were assessed by applying the Coats-Redfern method. The results obtained from this study will offer a reliable theoretical basis for optimizing the pyrolysis process.

2 Experimental

2.1 Proximate and ultimate analysis

The raw material used in this study is the tar generated by the fluidized-bed gasification of sawdust at 750°C. The biomass gasification condition can be seen from the reference[38]. Table 1

Received date: 2023-06-06 **Accepted date:** 2024-04-04

Biographies: Weijuan Lan, PhD, Associate Professor, research interest: clean energy technology, Email: lanwj2003@126.com; **Yunlong Zhou**, Graduate student, research interest: clean energy technology, Email: zhouyl1999@126.com; **Jiaxin Liu**, Graduate student, research interest: clean energy technology, Email: 3373339615@qq.com; **Yingxian Wang**, PhD, Lecturer, research interest: clean energy technology, Email: wyxian2021@163.com; **Dongxue Yin**, PhD, Associate Professor, research interest: clean energy technology, Email: milk2egg@163.com; **Jiangtao Ji**, PhD, Professor, research interest: agricultural engineering, Email: jjt0907@163.com.

***Corresponding author: Xin Jin**, Professor, research interest: agricultural engineering. College of Agricultural Equipment Engineering, Henan University of Science and Technology, Luoyang 471003, Henan, China. Tel:+86-18810559829, Email: jx.771@haust.edu.cn.

provides the elemental analysis of tar. As can be seen, the total contents of C, H, and O elements in tar exceeds 85% while N and S elements are relatively low, so little NO_X and sulfides are emitted during use.

Table 1 Ultimate analysis of tar

Sample	Characteristic contents/%							Calorific value
	Moisture	Ash content	C	H	N	S	O	MJ·kg^{-1}
Tar	15.90	0.10	60.79	6.68	1.79	0.09	20.33	25.501

2.2 Experimental methods and analysis

The ultimate analysis of tar was established using an Agilent 6890/5793N GC-MS system (Agilent Technologies, Santa Clara, CA, USA). The following GC conditions were used: 50°C for 5 min, and then heated to 250°C with a heating rate of 10 or 20°C/min. The MS conditions were as follows: ionization mode, EI; bombarding energy, 70 eV, mass scan range (m/z), 12 to approximately 550 amu, and split ratio, 80:1. To study the pyrolysis behavior, mechanism of tar degradation, and to establish the kinetic parameters of tar thermal decomposition, the TG analysis was performed on a WCT-1C thermal analyzer using an Al_2O_3 crucible (Xi'an Minx Testing Equipment Co., Ltd., Xi'an, China). The nitrogen was used as carrier gas while the sample mass was controlled in the range of 15-18 mg. First, the sample was placed in the crucible. Then, the N_2 was allowed to flow into the apparatus to eliminate the air. After that, the power of the thermal balance was switched on for heating. The sample was heated from room temperature to 750°C with two rates i.e., 10°C/min and 20°C/min while the gas flow of 50 mL/min.

3 Results and discussion

3.1 Chemical components of tar

Depending on the biomass materials, the operation parameters, process conversion devices used, and the purpose of experiment, the concentration of the main components of biomass tar are different[39]. However, it is universally recognized that the main components of bio-oil include acids, furans, and phenols while those of tar are represented by naphthalene and other macromolecular aromatic compounds, such as fluorene, phenanthrene, anthracene, pyrene, and other PAHs[40-43].

For this work, the selected tar to be studied was generated by biomass gasification at 750°C. The main components of the tar were identified and quantified by GC-MS. Figure 1 displays a representative total ion chromatogram registered for the tar under the conditions provided in the experimental part in which the relative abundances of the compounds are represented as a function of their retention time[44,45]. As shown, the components were well separated by the column. The identification of each peak, therefore for each element, was perfumed by comparison on NIST(Nationnal Institute of Standards and Technology) standard reference database and was based on the retention times. The results, which are in line with those previously published, show a complex chemical composition of the tar. Eighteen main compounds are listed in Table 2 alongside their retention times and chemical formula. It can be noticed that these compounds include phenol derivatives, naphthalene derivatives, other aromatic compounds, furans, and other compounds with carbon number between 7 and 20. Although complex, it can be observed that phenol (2), 4-ethyphenol (3), and n-pentadecane (13) are the most abundant components, followed by toluene (1), naphthalene-based compounds (5, 6, 7, and 10), furan-based compounds (11), or diphenyl derivatives (12). Therefore, the phenolic and furan-based compounds constitute the principal components of the tar obtained by biomass gasification at 750°C. However, despite their low contents, they were also identified among the essential components of tar.

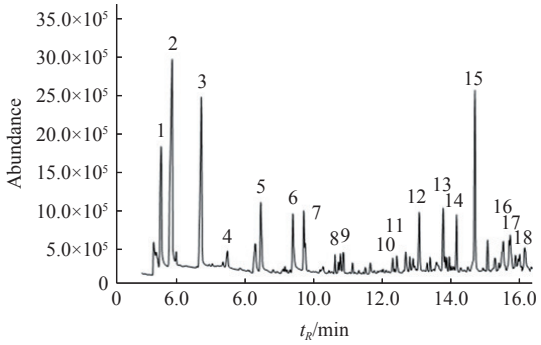

Figure 1 Total ion chromatogram of tar in biomass gasification

Table 2 The main compounds in tar

Component No.	Retention time/min	NIST98 library searching	Compound name	Molecular formula
1	5.800	Toluene	Toluene	C_7H_8
2	5.902	Phenol	Phenol	C_6H_6O
3	6.340	4-Ethyphenol	4-Ethyphenol	$C_8H_{10}O$
4	7.563	3-Ethyltoluene	3-Ethyltoluene	C_8H_{12}
5	8.205	Naphthalene	Naphthalene	$C_{10}H_8$
6	9.386	2-Methylcoumarone	2-Methylcoumarone	C_9H_8O
7	9.721	2-Methyl-naphthalene	2-Methyl-naphthalene	$C_{11}H_{10}$
8	10.471	Indene	Indene	C_9H_8
9	10.863	4-n-Propylphenol	4-n-Propylphenol	$C_9H_{12}O$
10	12.160	4-(2-Methoxyethyl) phenol	4-(2-Methoxyethyl) phenol	$C_9H_{12}O_2$
11	12.248	2-Methylindene	2-Methylindene	$C_{10}H_{10}$
12	13.010	Acenaphthylene	Acenaphthylene	$C_{12}H_8$
13	13.687	Dibenzofuran	Dibenzofuran	$C_{12}H_8O$
14	14.202	Diphenylenemethane	Diphenylenemethane	$C_{13}H_{10}$
15	14.600	n-Pentadecane	n-Pentadecane	$C_{15}H_{32}$
16	15.792	2-Methoxy	2-Methoxy	$C_{13}H_{10}O_2$
17	15.975	Naphthalene,1,5-dimethyl-	Naphthalene,1,5-dimethyl-	$C_{12}H_{12}$
18	16.218	Naphthalene,1,3-dimethyl-	Naphthalene,1,3-dimethyl-	$C_{12}H_{12}$

3.2 TG Analysis

The thermogravimetric analysis (TGA) of the tar was also performed to investigate the thermal behavior of the tar and to determine the activation energy of the tar degradation, based on the dynamic heating rate. The TG curves obtained by heating the sample from room temperature to 750°C with two heating rates i.e., 10°C/min and 20°C/min are shown in Figure 2. The corresponding derivative curves are also displayed in Figure 2.

As shown, three regions can be delimited for each TG curve regardless of the heating rate, suggesting a complex composition of tar, which includes compounds of different volatilities and thermal stabilities. The first stage (from room temperature to 105°C) displays a slow weight loss of tar during biomass gasification. From the analysis results of GC-MS, it can be observed that the first few compounds that appeared are all low molecular weight volatile compounds, such as toluene, phenols, etc. This indicates that the weight loss of tar at this time is related to the removal of low molecular weight volatile compounds, and the weight loss rate is about 10%. Yet, the corresponding weight loss and DTG peaks are slight. Therefore, the primary explanation for the weight loss within

this temperature interval is the volatilization of extremely volatile components into gaseous molecules, without any obvious thermal decomposition. When the temperature is less than 105°C, the volatile compounds of biomass tar start to precipitate, and, the higher the heating rate, the more obvious is the de-volatilization of volatiles.

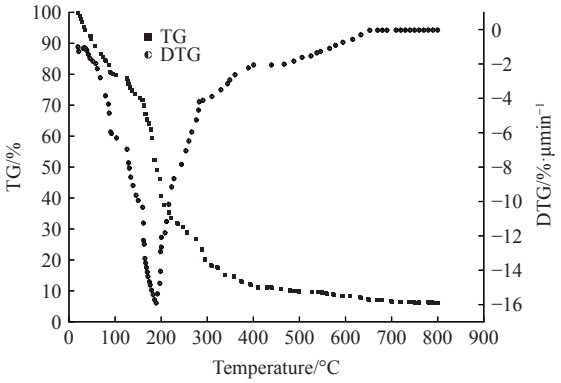

a. TG and DTG curves of tar obtained with 10 °C/min

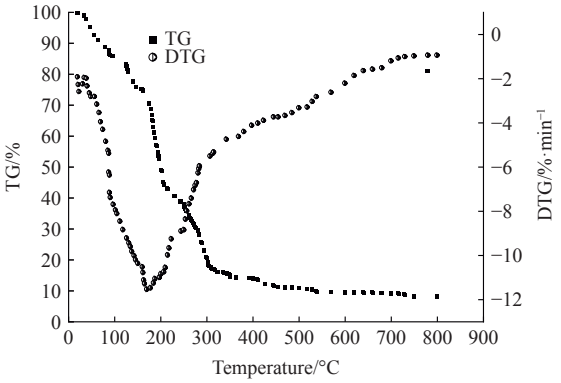

b. TG and DTG curves of tar obtained with 20 °C/min

Figure 2 TG and DTG curves of tar obtained with two heating rates

The second stage (105°C-380°C) is the main stage of the tar pyrolysis, when the most obvious weight loss is noticed. As the TG curves show, the most intense weight losses occur at about 200°C. Noticeably, the most intense peak in the DTG curves is at the same temperature, as well. This stage is related to the volatilization of high-boiling substances identified by GC-MS (such as naphthalene, esters, etc.), as well as the decomposition of some substances with poor thermal stability (such as dehydration of phenols and carboxyl decomposition of carboxylic acids), and the production of small gaseous molecules, such as CO_2, CO, H_2, CH_4, H_2O, etc. This is probably because, in this process, the main volatile matters of tar have precipitated. At the end of this interval, the TG curve is almost linear, suggesting that chemical compounds are already decomposed.

The interval from 380°C-750°C denotes the carbonization stage of biomass tar. In the first two stages of the thermal decomposition of tar, the weight loss of samples was 75%. In addition, during these two steps, a small amount of coke is generated as a result of the thermal decomposition of the organic compounds. Thus, the weight loss after 380°C is low. Normally, in this late stage of pyrolysis, biomass tar only contains coke, ash content, and a small amount of volatile matters. The low de-volatilization rate of volatile can be explained by the extremely low content of volatile matters. According to Figure 2, the weight loss rate gradually decreases to a constant level.

The following conclusions can be drawn from a comparison between TG and DTG curves:

When the heating rate increases, TG curve tends to move towards the high-temperature side, and gives rise to a temperature lag; in contrast, the peak temperature of DTG moves towards the high-temperature zone, and requires a higher pyrolysis temperature for the same weight loss. In other words, the peak temperature and maximum reaction rate of DTG curve both increased with the increasing heating rate. This is because, at different heating rates, heat is transferred from the outer wall of a sample towards its inside at different velocities as well. The magnitude of heating rate affects both the heat transfer velocity between sample crucible wall and sample, and that between outer sample and inner sample. When the heating rate is high, there is not enough time for samples to absorb the heat, so the temperature required by pyrolysis moves towards the high-temperature zone.

On the basis of the results provided by GC-MS and TG, a mechanism involved in the decomposition of tar is further proposed. Thus, it is suggested that, basically, the decomposition of the compounds constituting the tar follows a radical mechanism when the C-C bonds experience homolysis.

3.3 Kinetic investigations

The Coats-Redfern method is used for the analysis of the non-isothermal kinetics of tar based on the TG curve. As shown, the composition of tar is complex, and its pyrolysis process involves chemical reactions of a series of components. The DTG curve gives the global weight loss for all the decomposition reactions occurring in the pyrolysis process. The pyrolysis conversion rate, α, can be described by the weight change of samples according to the following expression[46,47]:

$$\ln\left[-\frac{\mathrm{d}\alpha}{\mathrm{d}T}\frac{1}{(1-\alpha)^n}\right]=\ln\frac{A}{\beta}-\frac{E}{RT} \quad (1)$$

where, n represents the reaction order. For a given heating rate $\beta=\frac{\mathrm{d}T}{\mathrm{d}t}$, (°C/min); t represents the reaction time, min; E represents the activation energy, kJ/mol; A represents the frequency factor (Arrhenius constant, min^{-1}); R denotes the universal constant of gases, (J/mol·K); T represents the temperature, K.

Assuming $Y=\ln\left[-\frac{\mathrm{d}\alpha}{\mathrm{d}T}\frac{1}{(1-\alpha)^n}\right]$, $X=\frac{1}{T}$, $a=-\frac{E}{R}$, $b=\ln\frac{A}{\beta}$, Equation (1) can be converted into:

$$Y=aX+b \quad (2)$$

Given $RT/E\ll 1$, α, and T obtained from TG curve, and reaction mechanism f_α and reaction order can be assumed before curve coupling. The value of linear correlation coefficient, R, is used as a criterion for judging whether the selected method to analyze data is suitable. After selecting a suitable method, E and A, can be solved from the slope and intercept of the line.

The α corresponds to different temperatures. T can be obtained from the TG curve. After plotting according to reaction rate and T^{-1}, E, and A are determined as mentioned above. As TG results showed, the weight loss of tar is a two-stage process. The first one is the removal of the volatile compounds (volatilization stage) while the second one is pyrolysis stage of heavy components. According to the experience summed up by our predecessors, set n=1, f_α=1–α, so that the function image of Y on the left side of Equation (2) vs X is approximately linear the values for E and A are listed in Table 3.

Table 3 *E* and *A* values of tar decomposition under different heating rates

Heating rate (β)/°C·min^{-1}	Reaction stage	Activation energy (E)/kJ·mol^{-1}	R	Frequency factor (A)/min^{-1}
10	Volatilization	96.350	0.9961	1.7×10^{5}
	Pyrolysis	62.100	0.9928	1.7×10^{3}
20	Volatilization	110.786	0.9968	4.1×10^{7}
	Pyrolysis	90.750	0.9838	9.1×10^{3}

As indicated by the data in Table 3, at the same heating rate, the activation energy changes from the volatilization to the pyrolysis stage, and E decreases as the temperature increases. However, when the heating rate changes, the activation energy for the same stage increases with an increase in the heating rate.

4 Conclusions

This study involved the analysis of the chemical composition of tar derived from biomass gasification using GC-MS. Furthermore, the decomposition kinetics of the tar was also studied by TG analysis. The following are the main findings of this work:

1) The GC-MS results showed that tar has a complex composition, which mainly includes phenol and its derivatives, naphthalene and its derivatives, and other macromolecular aromatic compounds (including phenol, naphthalene, and other PAHs), as well as furans and other compounds (carbon number: 7-14). It was also found that phenol, 4-ethyphenol, naphthalene, n-pentadecane, and toluene are present in high proportions in tar after biomass gasification. Overall, phenolic compounds are the main components of tar, and furans, despite their low contents, also constitute essential components of tar.

2) The degradation of tar is a two-step process, including a volatilization step at lower temperature (<105°C) and a pyrolysis step at higher temperatures (105°C-380°C). The activation energy for tar decomposition obtained from the TG curves registered at two heating rates (10°C/min and 20°C/min) and using Coats-Redfern model to interpret data increased for the same stage of decomposition as the heating rate was increased. Conversely, the activation energy decreased as the temperature enhanced at a constant heating rate.

Acknowledgements

This work was supported by the Key R&D Projects in Henan Province (Grant No. 241111321700); the Major Science and Technology Projects in Henan Province (Grant No. 231100110200), and the Key Scientific and Technological Project of Henan Province (Grant No. 232102240040, 232102110291).

[References]

[1] Inoue N, Tada T, Kawamoto K. Gas reforming and tar decomposition performance of nickel oxide (NiO)/SBA-15 catalyst in gasification of woody biomass. Journal of the Air & Waste Management Association, 2019; 69(4): 502–512.

[2] Yang H M, Liu J G, Zhang H, Han X X, Jiang X M. Experimental research for biomass steam gasification in a fluidized bed. Energy Sources, Part A: Recovery, Utilization, and Environmental Effects, 2019; 41(16): 1993–2006.

[3] Zhang J J, Wang M, Xu S P, Feng Y C. Hydrogen and methane mixture from biomass gasification coupled with catalytic tar reforming, methanation and adsorption enhanced reforming. Fuel Processing Technology, 2019; 192: 147–153.

[4] Xu G Y, Yang P, Yang S X, Wang H X, Fang B Z. Non-natural catalysts for catalytic tar conversion in biomass gasification technology. International Journal of Hydrogen Energy, 2022; 47(12): 7638–7665.

[5] Guo F Q, Liu Y, Wang Y, Li X L, Li T T, Guo C L. Pyrolysis kinetics and behavior of potassium-impregnated pine wood in TGA and a fixed-bed reactor. Energy Conversion and Management, 2016; 130: 184–191.

[6] Awais M, Li W, Arshad A, Haydar Z, Yaqoob N, Hussain S. Evaluating removal of tar contents in syngas produced from downdraft biomass gasification system. International Journal of Green Energy, 2018; 15(12): 724–731.

[7] Buentello-Montoya D, Zhang X L, Marques S, Geron M. Investigation of competitive tar reforming using activated char as catalyst. Energy Procedia, 2019; 158: 828–835.

[8] Saleem F, Zhang K, Harvey A. Plasma-assisted decomposition of a biomass gasification tar analogue into lower hydrocarbons in a synthetic product gas using a dielectric barrier discharge reactor. Fuel, 2019; 235: 1412–1419.

[9] Kobayashi J K, Kawamoto K, Kobayashi K. Effect of porous silica on the removal of tar components generated from waste biomass during catalytic reforming. Fuel Processing Technology, 2019; 194: 106104.

[10] Misse S E, Brillard A, Brilhac J-F, Obonou M, Ayina L M, Schönnenbeck C, et al. Thermogravimetric analyses and kinetic modeling of three Cameroonian biomass. Journal of Thermal Analysis and Calorimetry, 2018; 132: 1979–1994.

[11] Mureddu M, Dessì F, Orsini A, Ferrara F, Pettinau A. Air-and oxygen-blown characterization of coal and biomass by thermogravimetric analysis. Fuel, 2018; 212: 626–637.

[12] Li J, Chang G Z, Song K, Hao B L, Wang C P, Zhang J, et al. Influence of coal bottom ash additives on catalytic reforming of biomass pyrolysis gaseous tar and biochar/steam gasification reactivity. Renewable Energy, 2023; 203: 434–444.

[13] Valderrama Rios M L, González A M, Lora E E S, del Olmo O A A. Reduction of tar generated during biomass gasification: A review. Biomass & Bioenergy, 2018; 108: 345–370.

[14] Madav V, Das D, Kumar M, Surwade M, Parikh P P, Sethi V. Studies for removal of tar from producer gas in small scale biomass gasifiers using biodiesel. Biomass & Bioenergy, 2019; 123: 123–133.

[15] Shamsi M, Obaid A A, Farokhi S, Bayat A. A novel process simulation model for hydrogen production via reforming of biomass gasification tar. International Journal of Hydrogen Energy, 2022; 47(2): 772–781.

[16] Liang S, Guo F Q, Du S L, Tian B L, Dong Y C, Jia X P, et al. Synthesis of Sargassum char-supported Ni-Fe nanoparticles and its application in tar cracking during biomass pyrolysis. Fuel, 2020; 275: 117923.

[17] Li J, Jiao L G, Tao L Y, Chen G Y, Hu J L, Yan B B, et al. Can microwave treat biomass tar? A comprehensive study based on experimental and net energy analysis. Applied Energy, 2020; 272: 115194.

[18] Yin X F, He L M, Syed-Hassan S S A, Deng W, Ling P, Xiong Y M, et al. One-step preparation of a N-CNTs@Ni foam electrode material with the co-production of H_2 by catalytic reforming of N-containing compound of biomass tar. Fuel, 2020; 280: 118601.

[19] Chaurasia A. Modeling, simulation and optimization of downdraft gasifier: Studies on chemical kinetics and operating conditions on the performance of the biomass gasification process. Energy, 2016; 116: 1065–1076.

[20] Long Y Q, Li Q H, Zhou H, Meng A H, Zhang Y G. A grey-relation-based method (GRM) for thermogravimetric (TG) data analysis. Journal of Material Cycles and Waste Management, 2018; 20: 1026–1035.

[21] Tan R S, Abdullah T A T, Jalil A A, Isa K M. Optimization of hydrogen production from steam reforming of biomass tar over Ni/dolomite/La_2O_3 catalysts. Journal of the Energy Institute, 2020; 93(3): 1177–1186.

[22] Chen G Y, Liu C, Yan B B, Ma W C. Thermal Degradation behaviors and kinetics of biomass tar. Energy Procedia, 2014; 61: 1085–1088.

[23] Yu M M, Masnadi M S, Grace J R, Bi X T, Lim C J, Li Y H. Co-gasification of biosolids with biomass: Thermogravimetric analysis and pilot scale study in a bubbling fluidized bed reactor. Bioresource Technology, 2015; 175: 51–58.

[24] Guo F Q, Dong Y P, Fan P F, Lv Z C, Yang S, Dong L. Catalytic decomposition of biomass tar compound by calcined coal gangue: A kinetic study. International Journal of Hydrogen Energy, 2016; 41(31): 13380–13389.

[25] Xu T T, Xu F, Hu Z Q, Chen Z H, Xiao B. Non-isothermal kinetics of biomass-pyrolysis-derived-tar (BPDT) thermal decomposition via thermogravimetric analysis. Energy Conversion & Management, 2017; 138: 452–460.

[26] Velázquez-Martí B, Gaibor-Chavez J, Niño-Ruiz Z, Cortes-Rojas E. Development of biomass fast proximate analysis by thermogravimetric

scale. Renewable energy, 2018; 126: 954–959.
[27] Mallick D, Poddar M K, Mahanta P, Moholkar V S. Discernment of synergism in pyrolysis of biomass blends using thermogravimetric analysis. Bioresource Technology, 2018; 261: 294–305.
[28] Havilah P R, Sharma P K, Gopinath M. Combustion characteristics and kinetic parameter estimation of Lantana camara by thermogravimetric analysis. Biofuels, 2019; 10(3): 365–372.
[29] Silva J E, Calixto G Q, de Almeida C C, Melo D M A, Melo M A F, Freitas J C O, et al. Energy potential and thermogravimetric study of pyrolysis kinetics of biomass wastes. Journal of Thermal Analysis and Calorimetry, 2019; 137: 1635–1643.
[30] Umeda K, Nakamura S, Ding L, Yoshikawa K. Biomass gasification employing low-temperature carbonization pretreatment for tar reduction. Biomass & Bioenergy, 2019; 126: 142–149.
[31] Zeng X, Shen M J, Wang F, Ma X H, Hu D D, Wang T T, et al. Generation features and kinetics of gas products in bio-tar catalytic cracking by char for biomass gasification. International Journal of Hydrogen Energy, 2023; 48(82): 31905–31919.
[32] Zhu X F, Venderbosch R H. Experimental research on gasification of bio-oil derived from biomass pyrolysis. Journal of Fuel Chemistry and Technology, 2004; 32(4): 510–512. (in Chinese)
[33] Chen G Y, Li J, Cheng Z J, Yan B B, Ma W C, Yao J G. Investigation on model compound of biomass gasification tar cracking in microwave furnace: Comparative research. Applied Energy, 2018; 217: 249–257.
[34] Chen B, Shi Z M, Liu B, Jiang S J, He J Q. Combustion characteristics and combustion kinetics of gasification pine tar acted on by SiO_2. Journal of Central South University (Science and Technology), 2017; 48: 1936–1940.
[35] Wang S L, Zhang Q G, Li J H. Chemical composition of biomass tar and its distillations. Acta Energiae Solaris Sinica, 2006; 27: 647–651.
[36] Xie Q L, Borges F C, Cheng Y L, Wan Y Q, Li Y, Lin X Y, et al. Fast microwave-assisted catalytic gasification of biomass for syngas production and tar removal. Bioresource Technology, 2014; 156: 291–296.
[37] Karaosmanoglu F, Tetik E. Fuel properties of pyrolytic oil of the straw and stalk of rape plant. Renewable Energy, 1999; 16: 1090–1093.
[38] Lan W J, Chen G Y, Zhu X L, Wang X, Wang X T, Xu B. Research on the characteristics of biomass gasification in a fluidized bed. Journal of the Energy Institute, 2019; 92(3): 613–620.
[39] Qi G L. Experimental research and numerical simulation of biomass pyrolysis and tar thermal cracking. PhD dissertation. Harbin: Harbin Institute of Technology, 2010; 138 p. (in Chinese)
[40] Ninduangdee P, Kuprianov V I, Cha E Y, Kaewrath R, Youngyuen P, Atthawethworawuth W. Thermogravimetric studies of oil palm empty fruit bunch and palm kernel shell: TG/DTG analysis and modeling. Energy Procedia, 2015; 79: 453–458.
[41] Wang J X, Zhao H B. Thermogravimetric analysis of rubber glove pyrolysis by different iso-conversional methods. Waste and Biomass Valorization, 2015; 6(4): 527–533.
[42] Qiu S J, Chu H L, Zou Y J, Xiang C L, Zhang H Z, Sun L X, et al. Thermochemical studies of Rhodamine B and Rhodamine 6G by modulated differential scanning calorimetry and thermogravimetric analysis. Journal of Thermal Analysis and Calorimetry, 2016; 123(2): 1611–1618.
[43] Slezak R, Krzystek L, Ledakowicz S. Thermogravimetric analysis coupled with mass spectrometry of spent mushroom substrate and its fractions. Journal of Analytical and Applied Pyrolysis, 2018; 133: 1–8.
[44] Li X T, Grace J R, Lim C J, Watkinson A P, Chen H P, Kim J R. Biomass gasification in a circulating fluidized bed. Biomass & Bioenergy, 2004; 26(2): 171–193.
[45] Adamu S, Xiong Q G, Bakare I A, Hossain M M. Ni/$CeAl_2O_3$ for optimum hydrogen production from biomass/tar model compounds: Role of support type and ceria modification on desorption kinetics. International Journal of Hydrogen Energy, 2019; 44(30): 15811–15822.
[46] Zhao L X. Experimental study on high efficiency hydrogen production from biomass crude glycerol. PhD dissertation. Tianjin: Tianjin University, 2011; 04. 111p. (in Chinese)
[47] Cavattoni T, Garbarino G. Catalytic abatement of biomass tar: a technological perspective of Ni-based catalysts. Rendiconti Lincei, 2017; 28: 69–85.